INTERNATIONAL JOURNAL OF ENERGY STUDIES

Piezoelectric energy harvesting from vortex-induced vibrations on a GFRP beam with embedded piezoelectric patch

Hakan Uçar*

Design Project Office, 0000-0001-8602-801X

(*Corresponding Author:hakucar@ku.edu.tr)

Highlights

- PZT patches embedded into a GFRP composite are effective piezoelectric energy harvesters for harvesting energy from wind flow.

- Piezoelectric energy harvesters of this scale can be used especially in marine and aerospace platforms.

- Closeness of the vortex shedding frequency to the resonance frequency is critical in terms of voltage generation.

<u>**You can cite this article as:**</u> Ucar H. Piezoelectric energy harvesting from vortex-induced vibrations on a GFRP beam with embedded piezoelectric patch. Int J Energy Studies 2022; 7(2): 157-177.

ABSTRACT

In the present era, the demand for energy continues to increase and nevertheless, energy resources are gradually decreasing. Therefore, extracting energy from the operating ambient is of great importance especially for industrial applications. Among the numerous available ambient energy sources, wind energy is one of the most promising and prevalent energy sources existing in the environment. In this study, a piezoelectric energy harvester (PEH) consisting of an electromechanical coupling of GFRP cantilever beam with an embedded piezoelectric patch is developed for wind energy harvesting. The cantilever beam under the wind flow vibrates due to the pressure field that occurs on the leeward side of the beam. The generation of the pressure field is based on the vortex shedding phenomenon. Theoretical model of the regarding electromechanical coupling subjected to vortex induced vibration is presented and the effect of the pressure field having various vortex shedding frequencies on harvested power is investigated by means of numerical simulations validated with an experimental study. In order to determine the effect of the direction in which the wind excites the PEH, two wind flow conditions are considered; cross wind and head wind. According to the results, it was found that the PEH generates considerably more voltage outputs under cross wind loading than that obtained from the head wind excitation. In cross wind case, maximum open circuit voltage of 82.4 V is obtained at the wind speed of 6 m/s with the vortex shedding frequency of 18 Hz, which is very close to the second resonance frequency of the PEH. With a calculated load resistance of 100 kΩ, the resulting maximum direct voltage and electric power is 58.7 V and 11.5 mW, respectively. As far as the energy efficiency of PEH is concerned, it is determined that the efficiency is about 0.75 for the frequency of 18 Hz, which is quite acceptable for energy harvesting. It is concluded that a composite PEH with an embedded piezoelectric patch can be used as an effective energy harvester for the vortex induced vibration when the vortex shedding frequency is close to its resonance frequency.

Keywords: Energy harvesting, wind energy, piezoelectric material, vortex induced vibration, cross wind, head wind

1. INTRODUCTION

The past decades have seen an impressive rise in the research of energy harvesting from the environment due to the lack of natural energy resources. The concept of energy harvesting essentially involves the direct conversion of existing environmental energy into electrical energy by means of some particular mechanisms. Piezoelectric materials, such as lead zirconate titanate (PZT), play a critical role in harvesting energy due to their direct coupling properties, high energy density and ease of integration [1, 2]. Piezoelectric materials convert energy at a small scale and thus, the generated electrical outputs are expected to be used for powering low-power electronic devices.

The ambient energy exists in several forms such as fluid [3, 4], solar [5, 6], wind [7, 8], wave [9, 10] and vibration [11, 12]. Among them, owing to its wide availability, wind energy is one of the most promising energy sources existing in the environment. When structures are exposed to wind flows, undesired aeroelastic instabilities, such as flutter, galloping and vortex-induced vibration (VIV), will occur on the structure [13]. However, it may be possible to benefit from this unfavorable condition by harvesting energy from the structural vibration via piezoelectric materials. Numerous studies have been performed on the piezoelectric energy harvesting from wind energy. Among the studies based on flutter and galloping conditions, Liu et al. [14] proposed a piezoelectric energy harvester by using piezoelectric macro fiber composites based on the flutter mode. Macro fiber composites were selected due to their excellent flexibility on large deformations and it was concluded that the energy harvester based on flutter mode was effective in generating electrical outputs for conventional MEMS. In another flutter oscillation study, piezoelectric energy harvesting by a cantilever flag based on flutter mode and flutter instability of the flag subjected to axial flow were investigated [15]. Lim et al. [16] studied a piezoelectric cantilever beam with transverse galloping bluff body under natural wind condition. Different bluff body prisms such as square, triangle and D-section were studied under the natural wind condition and it was determined that higher power was obtained with the use of square prism as the bluff body.

For flutter and galloping conditions, a considerable energy can be harvested due to the self-excited vibration characteristics resulting in high amplitude vibrations [17, 18]. However, if the wind speed cannot be fully controlled, it is possible to encounter damage on the energy harvester. On the other hand, for the VIV based energy harvester case, there is a lock-in regime of wind speed where the vortex shedding frequency is locked with the resonance frequency of the structure.

Beyond this regime, the structural vibration starts to decrease and possible damage is prevented [19]. Akaydin et al. [20] experimentally investigated a VIV based piezoelectric energy harvester (PEH) subjected to a uniform and steady flow. Energy harvester was basically a cantilever beam having a cylinder attached to the free end and piezoelectric patches. Wu et al. [21] developed a VIV based PEH composed of a cantilever beam with piezoelectric patches and a proof mass. They investigated the effect of the length and location of the patches on the generated electrical outputs. A mathematical model of a piezoelectric cantilever beam with end mass vibrating under the influence of VIV was developed by Adhikari et al. [22]. In the study, energy harvester was subjected to random excitations instead of uniform and steady flow. Jia at al. [23] presented a detailed investigation on a novel asymmetric VIV based PEH for capturing wind energy at low wind speed. They concluded that the asymmetric energy harvester generated more power at low wind speed compared with conventional energy harvester. In another study, the effects of the Reynolds number on the piezoelectric energy harvesting from VIV of a circular cylinder were investigated by applying parametric study [24]. Mehdipour et al. [25] proposed a novel study for determining the best possible bluff body shape among several body shapes in different cross sections in order to enhance the low-speed VIV energy harvesting.

The main purpose of this study is to present a piezoelectric energy harvester with an embedded piezoelectric patch by combining the favorable mechanical properties of the GFRP material and VIV phenomenon. GFRP material is selected as the host material of the piezoelectric energy harvester due to its high strength to weight ratio, high durability and low stiffness compared to metals [26]. A PZT patch is embedded in the fixed end of the beam in order to provide a convenient protection against structural deformation and meteorological effects such as rain and humidity. In addition, the operability of PZT patches embedded in the composite is also investigated by an experimental study. Most PEH configurations use a bluff body attached at the free end. Herein this study, no bluff body is considered and two different wind loading cases are taken into account to determine the effect of the wind direction on energy harvesting. In the first case, the PEH is subjected to cross wind with various velocities resulting in VIV on the structure. Second case is the head wind acting through the cross section of the tip of PEH. Theoretical model considering VIV due to cross and head wind flows is introduced and energy harvesting simulations are performed based on vortex shedding frequencies.

2. MODELING PIEZOELECTRIC ENERGY HARVESTING FROM VORTEX-INDUCED VIBRATION

When a thin beam is subjected to steady and uniform wind flow, a vortex shedding phenomenon occurs on the leeward side of the beam. The formation of continuous alternating vortices in the downstream of the beam is called "vortex shedding". Under the vortex shedding excitations, the beam will be exposed to periodic oscillations, so called vortex induced vibration, resulting in a complex interaction between the beam and the vortices. In order to define the principle of a PEH exposed to wind flow, the dynamic response of the electromechanically coupled system under the wind flow with vortex shedding phenomenon is required. For this purpose, a mathematical model is created with respect to the harvester configuration and two wind flow cases, shown in Figure 1.
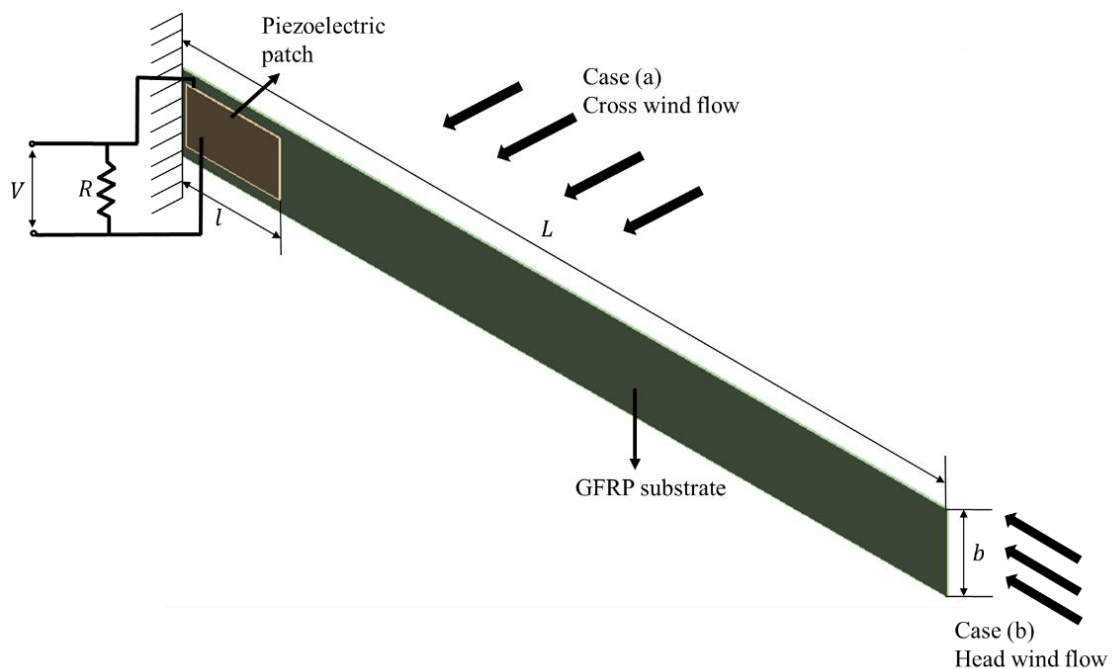
Figure 1. VIV based piezoelectric energy harvester

For thin beams, Euler–Bernoulli beam theory is commonly used to model the vibration of cantilever beams. As shown in Figure 1, the beam theory is applied in two sections separately since a piezoelectric patch is embedded at the fixed end and the material properties of coupled section differ from GFRP material which is used as the host material. According to the theory, the governing equations of the piezoelectric energy harvester regarding the sections with and without the piezoelectric patch can be expressed as:

for $(0 \leq x \leq l)$;

$$\left(E_h + E_p\right)I \frac{\partial^4 w(x,t)}{\partial x^4} + \left(\rho_h A_h + \rho_p A_p\right)\frac{\partial^2 w(x,t)}{\partial t^2} = F(t) \tag{1}$$

for $(l \leq x \leq L)$;

$$E_h I \frac{\partial^4 w(x,t)}{\partial x^4} + \rho_h A_h \frac{\partial^2 w(x,t)}{\partial t^2} = F(t) \tag{2}$$

where E_h and E_p is the Young's modulus of the beam material and piezoelectric material, respectively; A_h and A_p is the cross-section area of the beam and patch, respectively; ρ_h and ρ_p is the density of the beam material and piezoelectric material, respectively; *w(x, t)* is the dynamic displacement of the PEH; *I* is the second-moment of the cross-section given as $I = \frac{bt^3}{12}$, *t* is the thickness of the PEH. *F(t)* is the aerodynamic force per unit length exerted on the cantilever PEH due to the wind flow along with the vortex shedding, as expressed below [27].

$$F(t) = \frac{1}{2}\rho_a v^2 b C_L \sin \omega_s t \tag{3}$$

where ρ_a is the mass density of air; *v* is the wind velocity; ω_s is the vortex shedding frequency; C_L is the aerodynamic lift coefficient which is related to Reynolds number, wind velocity, angle of attack and the geometry of the structure. Lift coefficient is generally measured in a wind tunnel test set-up. In this study, it is computed with respect to Reynolds number and wind velocity by employing CFD simulations for each case.

When a wind flows through the PEH, the vortices start to form in its wake and shed into the downstream at the vortex shedding frequency, ω_s defined as;

$$\omega_s = 2\pi St \frac{v}{b} \tag{4}$$

where *St* is the Strouhal number and can be taken as 0.15 for the cross wind case and 0.06 for the head wind case with respect to the shape of the cross-section, as shown in Figure 2 [28, 29]. It should be noted that resonance condition can occur if the vortex shedding frequency is near the PEH's structural natural frequency.
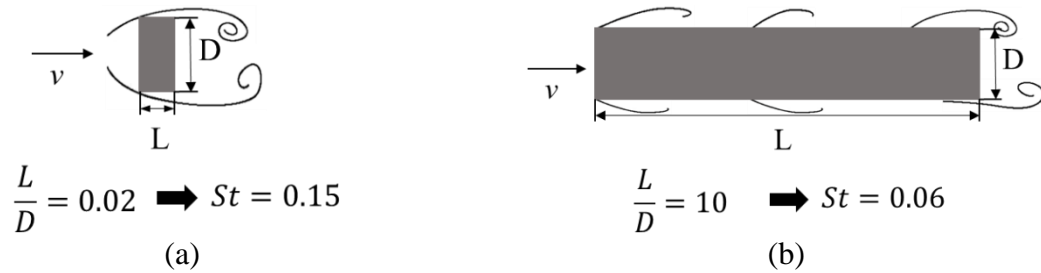
Figure 2. Vortex shedding and Strouhal number

(a) Case-1 Cross wind flow (b) Case-2 Head wind flow

Based on the modal transformation procedure, the vibration of the PEH can be represented as;

$$w(x,t) = \sum_{n=1}^{\infty} \emptyset(x,n). q_n(t) \tag{5}$$

where $\emptyset(x,n)$ is the mode shape of the PEH at its nth mode and $q_n(t)$ is the modal coordinate of the nth mode.

In order to determine the dynamic displacement as stated in Equation (1) and (2), the equation of motion should be rewritten in modal coordinates and the mode shapes should be identified assuming a free vibration.

or $(0 \leq x \leq l)$;

$$(E_h + E_p)I\frac{\partial^4 \emptyset_1(x)}{\partial x^4} - (\rho_h A_h + \rho_p A_p)\omega^2 \emptyset_1(x) = 0 \tag{6}$$

for $(l \leq x \leq L)$;

$$E_h I \frac{\partial^4 \emptyset_2(x)}{\partial x^4} - \rho_h A_h \omega^2 \emptyset_2(x) = 0 \tag{7}$$

where $\emptyset_1$ and $\emptyset_2$ is the corresponding mode shape functions for the sections with and without the piezoelectric patch, respectively. Free vibration solutions of the Equation (6) and (7) are obtained as;

$$\emptyset_1(x) = C_1 \cos \beta_1 x + C_2 \sin \beta_1 x + C_3 \cosh \beta_1 x + C_4 \sinh \beta_1 x \tag{8}$$

$$\emptyset_2(x) = C_5 \cos \beta_2 x + C_6 \sin \beta_2 x + C_7 \cosh \beta_2 x + C_8 \sinh \beta_2 x \tag{9}$$

where C_1 to C_8 are unknown constants and β_1 and β_2 are given as;

$$\beta_1 = \left(\frac{(\rho_h A_h + \rho_p A_p)\omega^2}{(E_h + E_p)I} \right)^{1/4} \tag{10}$$

$$\beta_2 = \left(\frac{\rho_h A_h \omega^2}{E_h I} \right)^{1/4} \tag{11}$$

The boundary and continuity conditions of PEH are given as follows, respectively.

$$\emptyset_1|_{x=0} \quad \left.\frac{d\emptyset_1}{dx}\right|_{x=0} = 0; \quad \left.\frac{d^2\emptyset_2}{dx^2}\right|_{x=L} = 0 \quad \left.\frac{d^3\emptyset_2}{dx^3}\right|_{x=L} = 0; \tag{12}$$

(at x=l) $\quad \emptyset_1 = \emptyset_2 ; \quad \dfrac{d\emptyset_1}{dx} = \dfrac{d\emptyset_2}{dx} ; \quad E_h I \dfrac{d^3\emptyset_2}{dx^3} = (E_h + E_p)I \dfrac{d^3\emptyset_1}{dx^3};$

$$\tag{13}$$

$$E_h I \frac{d^2\emptyset_2}{dx^2} = (E_h + E_p)I \frac{d^2\emptyset_1}{dx^2} + M_b,$$

where M_b is the bending moment occurred on the piezoelectric patch. For a thin beam, piezoelectric constitutive equations in the stress-displacement form is given as,

$$\begin{bmatrix} T_1 \\ D_3 \end{bmatrix} = \begin{bmatrix} c_{11}^E & -e_{31} \\ e_{31} & \varepsilon_{33}^T \end{bmatrix} \begin{bmatrix} S_1 \\ E_3 \end{bmatrix} \tag{14}$$

where T is the stress, S is the strain component, D is the electric displacement and E is the electric field component. Herein, c_{11}, e_{31}, ε_{33} are elastic, piezoelectric, and permittivity constants, respectively. Superscripts E and T state that the constants are evaluated at constant electric field and constant stress, respectively. According to the piezoelectric constitutive equation, M_b results in voltage generation, V_g as described [30],

$$V_g = -\frac{e_{31} b t}{2 C_v} \int_0^l \frac{d^2\emptyset_1}{dx^2} dx \tag{15}$$

where C_V is the electrical capacity of the piezoelectric patch.

Mode shape function, $\emptyset(x,n)$ can be derived by substituting Equation (8) and (9) into Equation (12) and (13) for each nth mode. On the other hand, the modal coordinate of the nth mode, $q_n(t)$ is determined as below,

$$q_n(t) = \frac{C_n}{B_n(\omega_n^2 - \omega_s^2)} F(t) \tag{16}$$

where

$$C_n = \omega_s^2 \int_0^L \emptyset(x,n)\, dx \tag{17}$$

$$B_n = \int_0^L \emptyset(x,n)^2\, dx \tag{18}$$

By applying the above mode shape function and modal coordinate solutions, the generated voltage with respect to time is obtained as;

$$V_g(t) = -\frac{e_{31}bt}{2C_v}F(t) \sum_{n=1}^{\infty} \frac{C_n}{B_n(\omega_n^2 - \omega_s^2)} \left(\frac{d\emptyset_1(x,n)}{dx}\bigg|_{x=L} - \frac{d\emptyset_1(x,n)}{dx}\bigg|_{x=0} \right) \tag{19}$$

Using the steady state expression of the generated voltage in Equation (19), the instantaneous power output, P(t) on the resistance can be calculated by employing

$$P(t) = \frac{V_g(t)^2}{R} \tag{20}$$

where R stands for the external resistance connected to the piezoelectric patch.

3. SIMULATIONS AND RESULTS

In this study, a cantilever beam composed of a GFRP substrate and an embedded piezoelectric patch is developed for harvesting energy from vortex induced vibrations due to the wind flow on the structure. Due to its corrosion resistance, high strength to weight ratio, high durability and low stiffness compared to metals, GFRP material is used as the material of the PEH substrate. PEH made of composite material will exhibit more deflection compared to that of metal PEH with same dimensions due to the lower stiffness value. Thus, more electrical energy outputs are aimed to be obtained from the composite PEH subjected to the wind loads. The energy harvesting capability of the PEH is investigated with different vortex shedding frequencies of cross wind and head wind

164

flows which are considered in order to determine the effect of the wind flow direction. A piezoceramic (PZT) patch, DuraAct PI P-876.A12, was utilized as piezoelectric material and embedded in the composite beam, as shown in Figure 3.(a), in order to investigate the applicability of PZT patches as built-in for composite structures and provide a convenient protection against structural and meteorological effects. Developed PEH is shown in Figure 3.(b) and the mechanical properties and dimension of PEH with respect to Figure 1 are given in Table 1.

In order to validate the numerical model of the PEH, an experimental study was conducted by applying a measurement set-up as shown in Figure 3.(c). Frequency responses as well as natural frequencies were obtained with the use of PZT patch and Laser Doppler Vibrometer (LDV). Elastic modulus of the GFRP material was derived by considering Euler-Bernoulli Beam Theory which presents the deflection characteristics of beams. Obtained values of the GFRP material were used in the numerical model and the measured frequency responses were compared with the calculated ones, as shown in Figure 4.
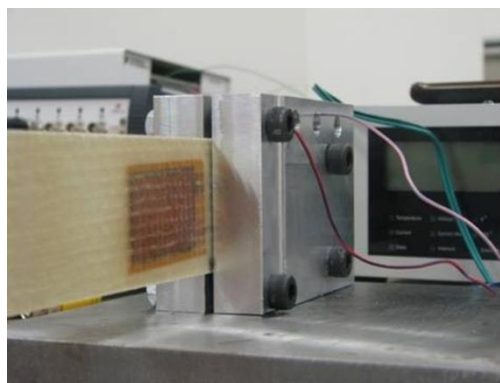
(a)
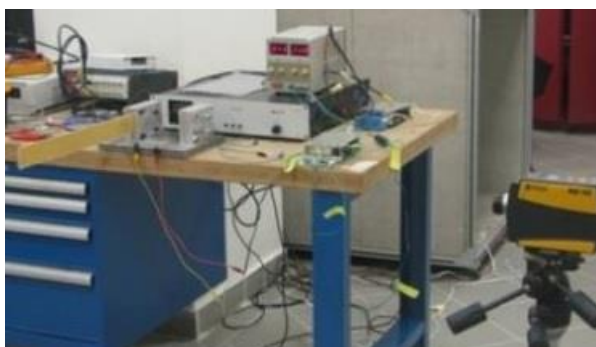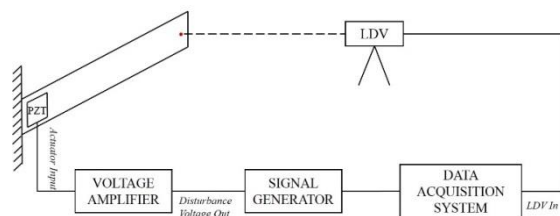
(b)   (c)

Figure 3. Cantilever PEH

(a) Embedded PZT patch, (b) Experimental set-up, (c) Measurement system

Table 1. Fundamental material properties and dimensions of PEH

Parameter	Substrate (GFRP)	Piezoelectric Patch (PZT)
L (mm)	500	-
l (mm)	-	61
b (mm)	50	45
t (mm)	1	0.8
ρ (kg/m^3)	2630	7800
E (GPa)	45	70.2
ζ	0.0176	-
d_{31} (pC/N)	-	-180
d_{33} (pC/N)	-	400
e_{33} (C/m^2)	-	13.814
$\varepsilon_{33}^T/\varepsilon_0$	-	1750
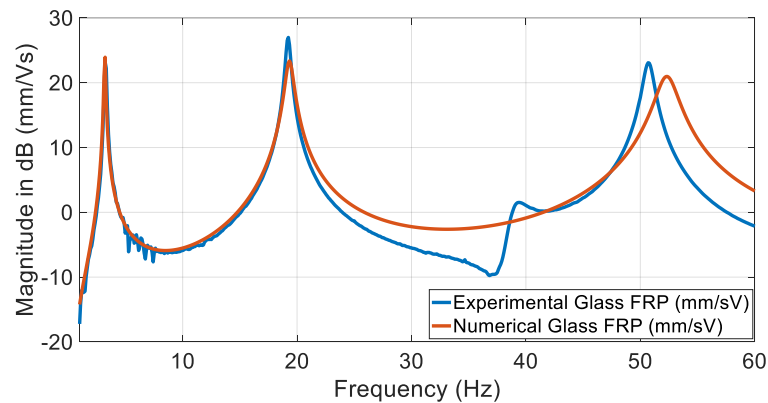
Figure 4. Frequency responses of PEH

As shown in Figure 4, first three resonance frequencies of PEH were determined as 3.19, 19.34 and 52.31 Hz, respectively and it should be noted that the numerical result matches well with the experimental one and therefore, the validated numerical PEH model can be utilized for energy harvesting study.

3.1. Generated Voltages

Open-circuit simulation was primarily carried out in order to determine the effective cross wind velocity to be used in harvesting energy for both cases. Under cross wind and head wind flows, the wind can possess the same vortex shedding frequency at different wind speeds due to the difference in Strouhal numbers. In this study, wind velocity from 0 to 45 m/s was taken into account and the vortex shedding frequency corresponding to each wind speed was calculated

according to Equation (4) considering both cases. The voltage outputs obtained in open-circuit operation with respect to vortex shedding frequencies are shown in Figure 5.
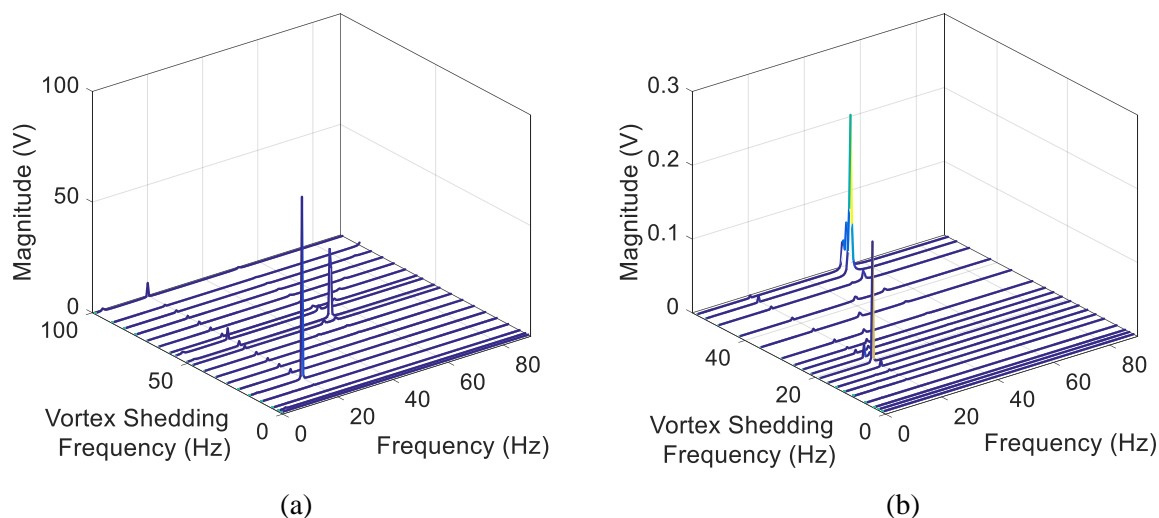
Figure 5. Open-circuit voltage generation with respect to vortex shedding frequencies.

(a) Cross wind case (b) Head wind case

As can be seen in Figure 5.(a), for cross wind case, it is determined that the maximum voltage is generated at the vortex shedding frequency of 18 Hz, which also corresponds to the second structural natural frequency ($\omega_{n=2} = 19.34$ Hz) of the PEH. Similarly, it is observed that considerable voltage is generated when the vortex shedding frequency is 51 Hz which is closer to the third natural frequency ($\omega_{n=3} = 52.31$ Hz) when compared with other frequency bands. Due to the resonance condition, high electrical outputs are obtained. On the other hand, it has been shown in Figure 5.(b) that the maximum voltage is obtained around the third mode of the PEH in the case of head wind loading. However, it is observed that the obtained voltage values are quite low compared to that of the cross wind case, as tabulated in Table-2. Besides, it should be noted that in the case of the head wind, the third mode dominates the energy harvesting, while in the case of the cross wind, the second mode dominates.

Table 2. Open-circuit voltage generation results

PEH Natural Frequency (ω_n-Hz)	Mode Shape	Case (a) Cross wind loadings		Case (b) Head wind loadings	
		Vortex Shedding Frequency (ω_s-Hz)	Generated Voltage (V)	Vortex Shedding Frequency (ω_s-Hz)	Generated Voltage (V)
19.34		18	82.4	19.2	0.163
52.31		51	30.8	51.6	0.216
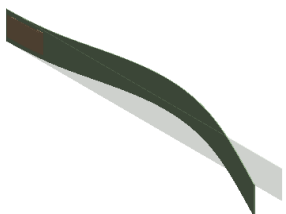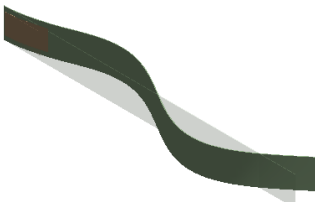
3.2. Harvested Power

Considering the voltage outputs obtained in both cases, only cross wind case was considered worth to be investigated in the power harvesting section. A defined resistive load, R is connected to the piezoelectric patch in order to obtain power. However, generated voltage by piezoelectric materials is sensitive to the attached resistors. In this part, vortex frequency of 18 Hz, corresponding to a wind velocity of 6 m/s at which the maximum voltage was generated, was taken into consideration for harvesting power. The resistive load was varied in a wide range from 10 Ω to 2 MΩ. Figure 6 presents the generated voltage with respect to attached resistive loads whereas generated peak voltage and power versus resistive load curve is shown in Figure 7.
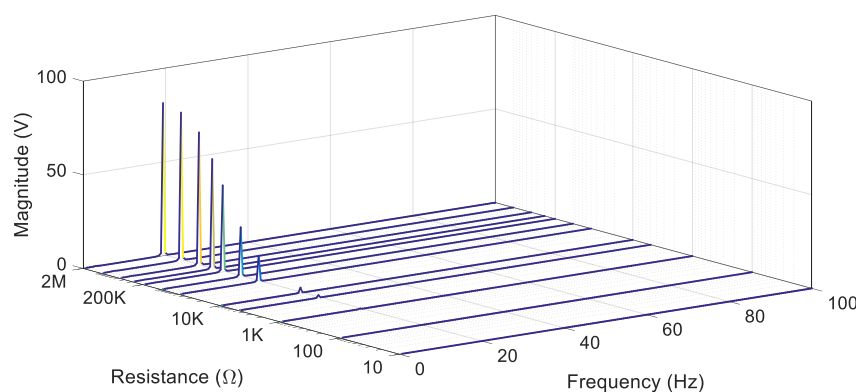
Figure 6. Generated voltage with respect to resistive loads when $\omega_s = 18\ Hz$
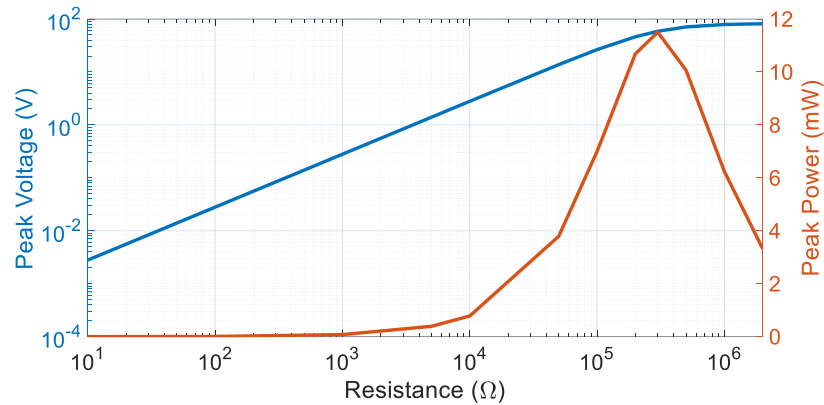
Figure 7. Peak electrical responses at PZT patch with respect to resistive loads.

As can be seen in Figure 7, after a resistive load case generated voltage remains almost constant whereas obtained power starts to decrease. Therefore, within the context of harvesting maximum power, the optimum resistive load should be properly selected with respect to the frequency of interest. Maximum power generation is attainable when the load impedance and the internal impedance of the harvester are equal to each other. The procedure of determining the optimum resistive load is called resistive impedance matching and the optimum resistive load can be calculated by using Equation (21) [31].

$$R_{opt} = \frac{1}{2\pi f C_p} \tag{21}$$

where C_p is the internal capacitance of the piezoelectric material, f is the excitation frequency. For the PZT patch used in this study, R_{opt} is calculated as 100 kΩ since the frequency of interest is determined as 18 Hz in the open-circuit analysis. Figure 8 presents the harvested power with respect to attached optimum resistive load when the cross wind velocity is 6 m/s with a vortex shedding frequency of 18 Hz which is very close to the resonance frequency of PEH. At the optimal resistive load value of 100 kΩ, a maximum voltage of 58.7 V with a harvested power of 11.5 mW is obtained.
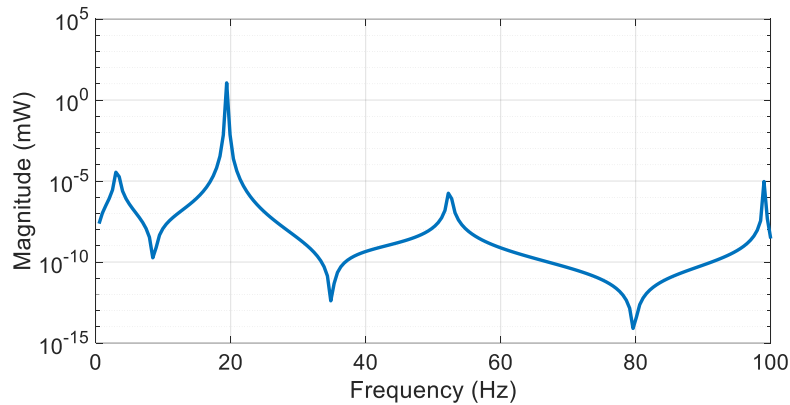
Figure 8. Harvested power with respect to R_{opt}=100 kΩ resistive loads when $\omega_s = 18\,Hz$

According to the results, the energy harvesting efficiency of PEH increases remarkably when the vortex shedding frequency is close to the resonance frequency of PEH. Besides, it should be noted that the maximum mechanical strain on the PEH with a harvested power of 11.5 mW is calculated as 2 mm/mm.

3.3. PEH Efficiency

Efficiency, also called energy conversion efficiency, is described as the ratio between the useful output energy and the input energy of a system. For PEH, it can be defined as the ratio of the output electrical energy to the input mechanical energy. This definition is similar to the electromechanical coupling factor squared, k_{ij}^2 , where k_{ij} is the material coupling factor (electrical field in direction i, stress in direction j). This factor is supplied by the piezoelectric material manufacturers and represents the efficiency of the piezoelectric material alone in converting mechanical energy into electrical energy. Thus, material coupling factor, k_{ij} does not consider the structural design as well as rectification circuit and cannot be applied to the entire PEH. The overall PEH efficiency is generally much smaller than the material coupling factor, k_{ij}. [32]

Many expressions for the input and output energy have been defined in the efficiency calculation for PEH. Among them, Shu and Lien [33] theoretically analyzed the energy conversion efficiency of a cantilever PEH and assumed that the input energy was the sum of obtained electrical energy and the dissipated energy by the structural damping. Thus, the energy conversion efficiency is calculated by

$$\eta = \frac{\alpha\kappa^2}{\zeta(\alpha\widetilde{\omega} + \pi/2)^2 + \alpha\kappa^2} \tag{22}$$

$$\alpha = \frac{1}{RC_p\omega_n} \tag{23}$$

where α is the normalized resistance (load resistance/matching resistance), $\widetilde{\omega}$ is the ratio between the response frequency and natural frequency, κ^2 is the electromechanical coupling coefficient and ζ is the structural damping ratio. The efficiency expression states that the efficiency increases with a large electromechanical coupling coefficient and a small damping ratio. Therefore, designs with thin films and small internal capacitance have proven to be more efficient, as the electromechanical coupling coefficient is inversely proportional to the stiffness and piezoelectric internal capacitance [34]. Electromechanical coupling coefficient, κ^2 can be calculated based on the expressions below.

$$\kappa^2 = \frac{\theta^2}{kC_p} \tag{24}$$

$$\theta^2 = b^2 t^2 e^2 \left(1 - \frac{r}{2}\right)^2 \left(\frac{3}{2l}\right)^2 \tag{25}$$

$$k = \frac{E_p bt^3}{4l^3}(r^3 - 3r^2 + 3r) + \frac{E_h bt^3}{4L^3}(1 - r)^3 \tag{26}$$

where r is the ratio between the thickness of the piezoelectric layer and the beam thickness ($r = t_p/t$), k is the stiffness, θ is the piezoelectric coupling factor, ε^S is piezoelectric permittivity constant evaluated at constant strain, and e is the piezoelectric stress constant. It can be observed that the coupling coefficient is independent of all beam properties other than the thickness ratio and material properties [35]. As stated in Section 3.2, the maximum electric power is extracted by the external electrical load at the impedance matching condition. For different exciting frequencies, the resistive load should be adjusted accordingly, which results in considerable time and huge efforts. Therefore, a fixed optimum resistance is generally used. In this study, fixed R_{opt}=100 kΩ is considered since the frequency of interest is 18 Hz and calculated PEH efficiency is shown in Figure 9. According to the figure, it can be stated that the efficiency of the PEH for the exciting frequency of 18 Hz is about 0.75. According to Eq. (22) and (23), one of the parameters

that affects the efficiency is the resistive load. As shown in Figure 10, the efficiency increases as the resistive load increases and it attains the peak value around the matching resistance point (R_{opt}= 100 kΩ) and then reduces significantly.
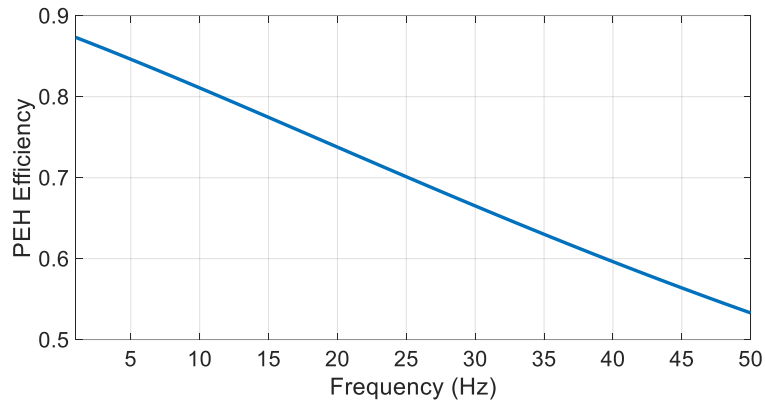
Figure 9. PEH efficiency with different frequencies
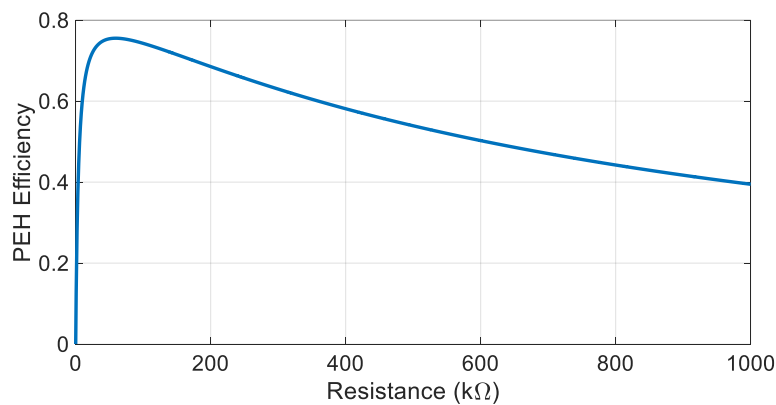
Figure 10. Effect of the resistive load on efficiency (at $\widetilde{\omega}$=1)

4. CONCLUSION

The main objective of this study is to investigate the energy harvesting capability of a newly designed cantilever PEH exposed to the wind flow. Distinctly from common PEH designs, a PEH, composed of a host structure made of GFRP composite and a PZT patch embedded in the composite, is developed. In this configuration, the bluff body is not applied on the PEH. Owing to the low stiffness and high corrosion resistance properties of GFRP, high deflection is achieved and resistance to atmospheric conditions is provided, respectively. On the other hand, the embedded condition of PZT provides considerable protection against structural deformation as well as meteorological effects such as humidity and rain.

A comprehensive numerical model is presented to calculate the dynamic behavior of the PEH as well as the generated electrical outputs with respect to different wind velocities. An experimental study was performed and the frequency response and natural frequencies of the structure were obtained. After a proper numerical validation, wind flow was applied to the PEH at vortex shedding frequencies with different wind speeds and different wind directions. and energy harvesting capability of the PEH was investigated.

Considering a particular wind flow with variable wind velocities, it is found that the wind velocity is critical in terms of energy harvesting since it defines the vortex shedding frequency along with the geometry of the PEH. Higher electrical outputs can be obtained while the vortex shedding frequency is close to the natural frequency of the PEH. Thus, it can be stated that piezoelectric energy harvesting based on VIV is efficient at resonance condition between the vortex shedding frequency and structural resonance frequency. In cross wind case, maximum open circuit voltage of 82.4 V is obtained at the wind speed of 6 m/s with the vortex shedding frequency of 18 Hz which is very close to the second resonance frequency of the PEH. On the other hand, in head wind case 0.216 V maximum voltage is generated at the wind speed of 43.6 m/s corresponding to vortex shedding frequency of 52.31 Hz which is very close to the third resonance frequency of the PEH. It is determined that considerably more voltage is generated in the case of cross wind compared to that obtained from the head wind case and a higher wind velocity is required to generate voltage under the head wind condition. As for power harvesting, with a calculated load resistance of 100 kΩ, the resulting maximum direct voltage and electric power is 58.7 V and 11.5 mW, respectively for the cross wind case. The harvested power is found to be sufficient to power low-power devices such as wireless sensors and microelectronics.

Energy efficiency of PEH in converting mechanical energy to electrical energy dissipated by a load resistance is also investigated. According to calculations, the efficiency of presented PEH for a wind speed of 6 m/s with the vortex shedding frequency of 18 Hz is found to be 0.75, which can be named to be quite efficient. Furthermore, it should be noted that the best efficiency can be obtained at resonance condition with the optimal resistive load.

As a consequence, it can be stated that the presented PEH, consisting of an embedded PZT patch and GFRP composite that supplants metals with its many properties along with its resistance to atmospheric conditions, is an effective tool for harvesting energy from wind flows and PZT

patches can be utilized as built-in for composite structures. While PEHs of this scale can be used especially in marine and aerospace platforms, higher electrical outputs can be obtained in land facilities having the presented PEHs with larger scales.

ACKNOWLEDGMENT

DECLARATION OF ETHICAL STANDARDS

The author of the paper submitted declare that nothing which is necessary for achieving the paper requires ethical committee and/or legal-special permissions.

CONTRIBUTION OF THE AUTHORS

Hakan Ucar: Performed the experiments, analyse the results and wrote the manuscript.

CONFLICT OF INTEREST

There is no conflict of interest in this study.

REFERENCES

[1] Erturk A, Inman DJ. Piezoelectric energy harvesting. John Wiley & Sons, US, 2011.

[2] Covaci C, Gontean A. Piezoelectric energy harvesting solutions: A review. Sensors; 2020; 20:3512.

[3] Aranda JJL, Bader S, Oelmann B. A space-coiling resonator for improved energy harvesting in fluid power systems. Sens. Actuators A: Phys. 2019; 29:58–67.

[4] Wang J, Zhao G, Xu J, Duan K, Zhang M, Zhu H. Numerical analysis of hydroenergy harvesting from vortex-induced vibrations of a cylinder with groove structures. Ocean Engineering 2020; 218:108219.

[5] Song YS, Youn JR, Yu C, Park J. Sustainable solar energy harvesting using phase change material (PCM) embedded pyroelectric system. Energy Conversion and Management 2022; 253:115145.

[6] Zhao YN, Li ML, Long R, Liu ZC, Liu W. Dynamic modeling and analysis of an advanced adsorption-based osmotic heat engines to harvest solar energy. Renewable Energy 2021; 175:638–649. https://doi.org/10.1016/j.renene.2021.05.010.

[7] Jing B, Hao W. Vibration analysis of rotting wind blades based on piezoelectric materials. International Journal of Acoustics and Vibration 2020; 26, 1:49-55.

[8] Zhou Z, Pan J, Qin W, Zhu P, Zhang H, Du W, Deng W. Improve efficiency of harvesting wind energy by integrating bi-stability and swinging balls. Mechanical Systems and Signal Processing 2022; 170:108816.

[9] Han J, Maeda T, Itakura H, Kitazawa D. Experimental study on the wave energy harvesting performance of a small suspension catamaran exploiting the maximum power point tracking approach. Ocean Engineering 2022; 243:110176.

[10] Ucar H. Patch-based piezoelectric energy harvesting on a marine boat exposed to wave-induced loads.Ocean Engineering 2021; 236: 109568.

[11] Pereira JC, Morangueira YLA. Energy harvesting assessment with a coupled full car and piezoelectric model. Energy 2020; 210:118668.

[12] Qin W, Pan J, Deng W, Zhang P, Zhou Z. Harvesting weak vibration energy by integrating piezoelectric inverted beam and pendulum. Energy 2021; 227:120374.

[13] Zhao L, Yang Y. On the modeling methods of small-scale piezoelectric wind energy harvesting. Smart Struct Syst 2017; 19(1):67–90.

[14] Liu J, Zuo H, Xiao W, Luo Y, Yaob D, Chena Y, Wanga K, Li Q. Wind energy harvesting using piezoelectric macro fiber composites based on flutter mode. Microelectronic Engineering 2020; 231:111333.

[15] Eugeni M, Elahi H, Fune F, Lampani L, Mastroddi F, Romano GP, Gaudenzi P. Numerical and experimental investigation of piezoelectric energy harvester based on flag-flutter. Aerospace Science and Technology 2020; 97:105634.

[16] Lim YY, Padilla RV, Unger A, Barraza R, Thabet AM, Izadgoshasb I. A self-tunable wind energy harvester utilising a piezoelectric cantilever beam with bluff body under transverse galloping for field deployment. Energy Conversion and Management 2021; 245:114559.

[17] Barrero-Gil A, Vicente-Ludlam D, Gutierrez D, Sastre F. Enhance of energy harvesting from transverse galloping by actively rotating the galloping body. Energies 2020; 13(1):91.

[18] Sun W, Jo S, Seok J. Development of the optimal bluff body for wind energy harvesting using the synergetic effect of coupled vortex induced vibration and galloping phenomena. International Journal of Mechanical Sciences 2019; 156:435–445.

[19] Dai H, Abdelkefi A, Wang L. Theoretical modeling and nonlinear analysis of piezoelectric energy harvesting from vortex-induced vibrations. Journal of Intelligent Material Systems and Structures 2014; 25 (14):1861–1874.

[20] Akaydin HD, Elvin N, Andreopoulos Y. The performance of a self-excited fluidic energy harvester. Smart Materials and Structures 2012; 21(2):025007.

[21] Wu N, Wang Q, Xie X. Wind energy harvesting with a piezoelectric harvester. Smart Materials and Structures 2013; 22:095023.

[22] Adhikari S, Rastogi A, Bhattacharya B. Piezoelectric vortex induced vibration energy harvesting in a random flow field. Smart Materials and Structures 2020; 29:035034.

[23] Jia J, Shan X, Upadrashta D, Xie T, Yang Y, Song R. An asymmetric bending-torsional piezoelectric energy harvester at low wind speed. Energy 2020; 198:117287.

[24] Zhang M, Zhang C, Abdelkefi A, Yu H, Gaidai O, Qin X, Zhu H, Wang J. Piezoelectric energy harvesting from vortex-induced vibration of a circular cylinder: Effect of Reynolds number. Ocean Engineering 2021; 235:109378.

[25] Mehdipour I, Madaro F, Rizzi F, De Vittorio M. Comprehensive experimental study on bluff body shapes for vortex-induced vibration piezoelectric energy harvesting mechanisms. Energy Conversion and Management: X 2022; 13:100174.

[26] Rajak DK, Pagar DD, Menezes PL, Linul E. Fiber-reinforced polymer composites: manufacturing, properties, and applications. Polymers 2019;11:1667.

[27] White FM. Fluid Mechanics 5th edn. McGraw Hill, New York, US, 2003.

[28] European Standards 1978 Recommendations for the Calculation of Wind Effects on Buildings and Structures (Brussels: European Committee for Structural Steelwork (ECSS))

[29] American National Standards Institute 1982 Minimum Building Loads for Buildings and Other Structures (New York: American National Standards Institute)

[30] Lin CC, Hsu CY. Static shape control of smart beam plates laminated with sine sensors and actuators. Smart Materials and Structures 1999; 8:519–530.

[31] Chandwani J, Somkuwar R, Deshmukh R. Multi-band piezoelectric vibration energy harvester for low-frequency applications. Microsystem Technologies 2019;25:3867–3877.

[32] Yang ZB, Erturk A, Zu J. On the efficiency of piezoelectric energy harvesters. Extreme Mechanics Letters 2017; 15: 26-37.

[33] Shu Y, Lien I. Efficiency of energy conversion for a piezoelectric power harvesting system. Journal of Micromechanics and Microengineering 2006; 16 (11): 2429.

[34] Stamatellou AM, Kalfas AI. On the efficiency of a piezoelectric energy harvester under combined aeroelastic and base excitation. Micromachines 2021; 12, 962.

[35] Shafer MW, Bryant M and Garcia E. Designing maximum power output into piezoelectric energy harvesters. Smart Materials and Structures 2012; 21: 109601.